Available online at www.sciencedirect.com
ScienceDirect
Ceramics International 37 (2011) 513–519
CERAMICS INTERNATIONAL
www.elsevier.com/locate/ceramint

Optical properties of Er,Yb co-doped YAG transparent ceramics

Jun Zhou [a,b], Wenxin Zhang [a,b], Tongde Huang [c], Liang Wang [a,b], Jiang Li [a], Wenbin Liu [a], Benxue Jiang [a], Yubai Pan [a,*], Jingkun Guo [a]

[a] Key Laboratory of Transparent and Opto-functional Advanced Inorganic Materials, Shanghai Institute of Ceramics, Chinese Academy of Sciences, 1295 Ding Xi Road, Shanghai 200050, China
[b] Graduate School of the Chinese Academy of Sciences, 19A Yuquan Road, Beijing 100039, China
[c] The Hong Kong University of Science and Technology, Clear Water Bay, Kowloon, Hong Kong

Received 7 May 2010; received in revised form 19 June 2010; accepted 21 September 2010
Available online 28 October 2010

Abstract

The transparent polycrystalline erbium and ytterbium co-doped yttrium aluminum garnet (Er,Yb:YAG) ceramics with various Yb contents from 5% to 25% were prepared by the solid-state reaction and the vacuum-sintering technique. The in-line transmittances of the mirror-polished ceramics exceed 80% from the visible band to the infrared band. The samples are very compact with few pores. The average grain size of the Er,Yb:YAG ceramic is about 15 μm. The upconversion luminescence spectra, infrared luminescence spectra and luminescence decay curves of the ceramics were observed and discussed. For 1%Er doped YAG ceramic, the best ion ratio of Yb^{3+} and Er^{3+} is around 15:1.

Keywords: C. Optical properties; Transparent ceramics; Er; Yb

1. Introduction

The Er doped transparent materials are essential for obtaining 1.5–1.65 μm lasers, which are widely utilized for long-distance telemetry and ranging based on considerations of atmospheric transparency and eye safety. Due to the three energy levels of the laser system and low absorption of Er^{3+} ions to the pump sources, it is difficult to increase the laser output efficiency. A significant way to increase the output efficiency is improving the absorption to the pump sources. Fortunately, Yb^{3+} ions are possessed of excellent ability of absorbing the lights between 900 and 1000 nm and then transferring the energy to Er^{3+} ions through the direct energy transfer (DT) from $^2F_{5/2}$ level of Yb^{3+} to $^4I_{11/2}$ level of Er^{3+}. So the Er,Yb co-doped optical materials have been widely studied [1–6]. However, the applications of Er lasers are still limited because of the poor chemical stability and low laser induced damage threshold of the glass hosts. Moreover, the steps of searching for new host materials have never stopped. Since Japanese scientists successfully fabricated Nd doped polycrystalline yttrium aluminum garnet with nearly the same optical properties as those of single crystal YAG and performed oscillation experiments with the laser diode (LD) excitation system using the Nd:YAG ceramics in 1995 [7], the polycrystalline ceramics have been rapidly developed and have become very important laser host materials to widen the fields of laser applications [8–16]. The diode-pumped Nd:YAG, Yb:YAG and composite YAG/Nd:YAG/YAG ceramics laser experiments have been successfully performed [12–16] and other garnet structure ceramics (i.e. TmAG [17]) have been fabricated in our group. Compared with the single crystals, ceramics have many advantages, such as ease of fabrication, less cost, large sizes, multifunctional structures, and mass production. Although the 1.65 μm laser experiment with an output pulse energy of 80 mJ and an optical slope efficiency of 3.4% has been performed using single crystal Er,Yb:YAG in 2005 [18], it is still very significant to study Er,Yb co-doped YAG ceramics. In the present work, Er,Yb:YAG transparent ceramics were fabricated for the laser experiments around 1.5 μm in the future. The upconversion luminescence spectra, infrared luminescence spectra and luminescence decay curves of the ceramics were observed and discussed.

* Corresponding author. Tel.: +86 21 52412820; fax: +86 21 52413903.
E-mail address: ybpan@mail.sic.ac.cn (Y. Pan).

0272-8842/$36.00
doi:10.1016/j.ceramint.2010.09.031

Fig. 1. The appearances of the Er,Yb:YAG ceramics mirror-polished on both surfaces.

2. Materials and methods

The commercial high-purity α-Al_2O_3 (>99.99%), Y_2O_3 (>99.99%), Er_2O_3 (>99.99%) and Yb_2O_3 (>99.99%) powders were used as starting materials. These powders were weighed according to the stoichiometric ratios of the Er,Yb:YAG ceramics and milled using Al_2O_3 balls for 12 h with ethanol as the milling medium and tetraethyl orthosilicate as the sintering additive. After fully dried and sieved through 200-mesh screen, the powder mixtures were dry-pressed under 80–100 MPa to form disks and then isostatically cold-pressed under 250 MPa. The powder compacts were vacuum-sintered at 1800 °C for 20 h under 10^{-3} Pa and then fully annealed at 1550 °C for 10 h under atmosphere.

To measure the grain sizes, the cylinder samples were mirror-polished and then etched at 1550 °C for 2 h under atmosphere. The surface microstructures were observed by the electron probe micro-analyzer (EPMA) (Model JSM-6700, JEOL, Tokyo, Japan). The samples (thickness = 2 mm) mirror-polished on both surfaces were used to measure in-line optical transmittances (Model U-2800 Spectrophotometer, Hitachi, Tokyo, Japan). To measure the luminescence spectra and luminescence decay curves (Fluorolog-3, Jobin Yvon, Paris, France; Hamamsatsu R5509-72 detector), the samples were excited with a 940 nm LD.

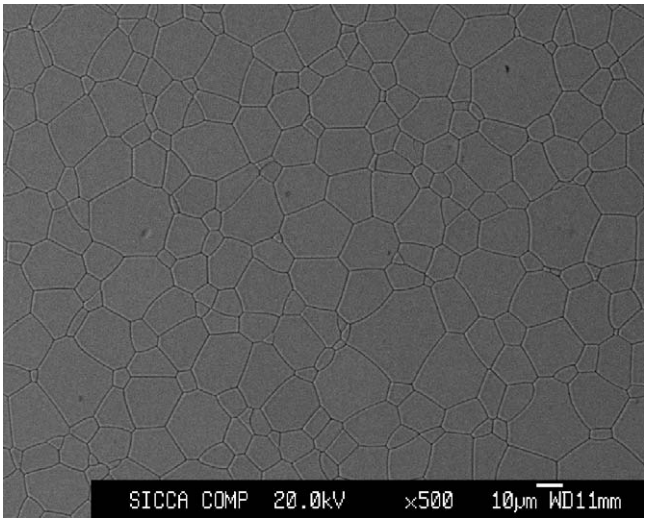

Fig. 2. The EPMA photograph of the 1%Er,5%Yb:YAG ceramics microstructure.

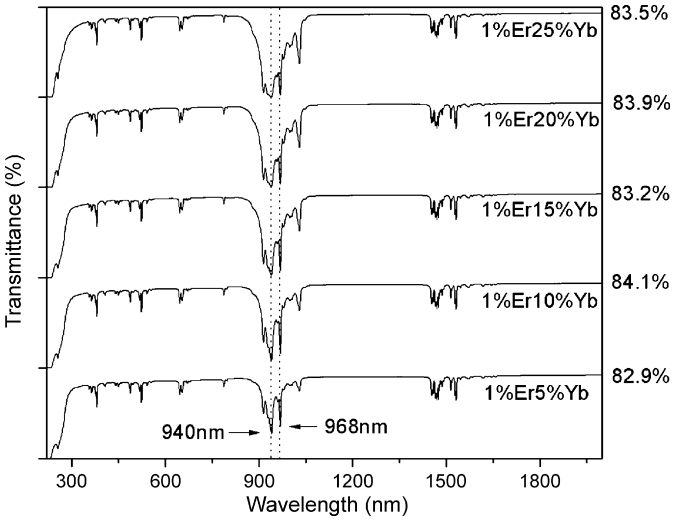

Fig. 3. The in-line transmittance curves of the mirror-polished Er,Yb:YAG ceramics under room temperature (thickness = 2 mm).

3. Results and discussion

The Er,Yb:YAG ceramics with various Yb contents (1%Er–5%Yb, 1%Er–10%Yb, 1%Er–15%Yb, 1%Er–20%Yb and 1%Er–25%Yb) were prepared by the above method. The ceramics with different sizes are shown in Fig. 1. It can be seen that the ceramics with different Yb contents share the same appearances because Yb^{3+} ions have no absorption peaks in the visible band.

Fig. 2 shows the EPMA photograph of the 1%Er,5%Yb:YAG ceramic. It can be seen that the sample is very compact almost without pores and secondary phases both at the grain boundaries and in the grains. The average grain size of the

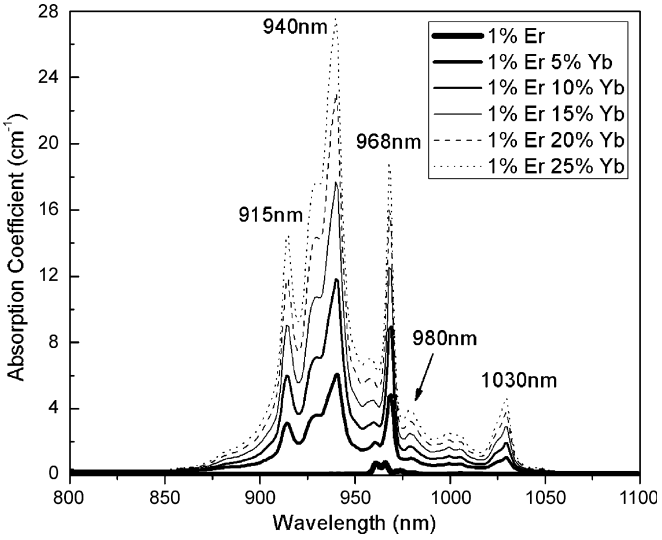

Fig. 4. The absorption coefficient curves of the Er,Yb:YAG ceramics under room temperature.

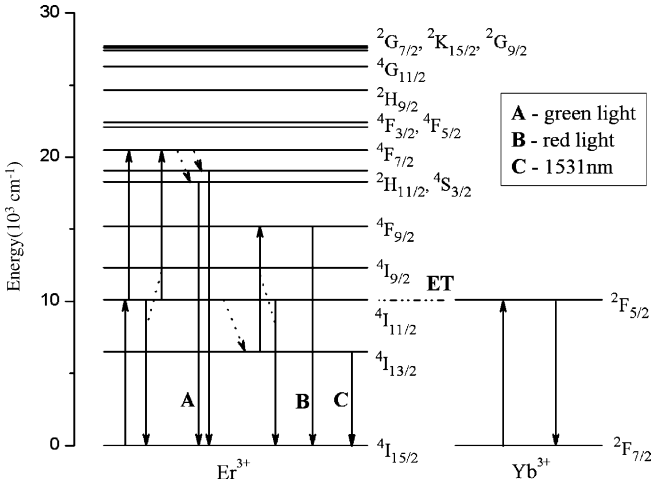

Fig. 5. The energy level diagram of Er,Yb co-doped materials under excitation of the 940 nm LD.

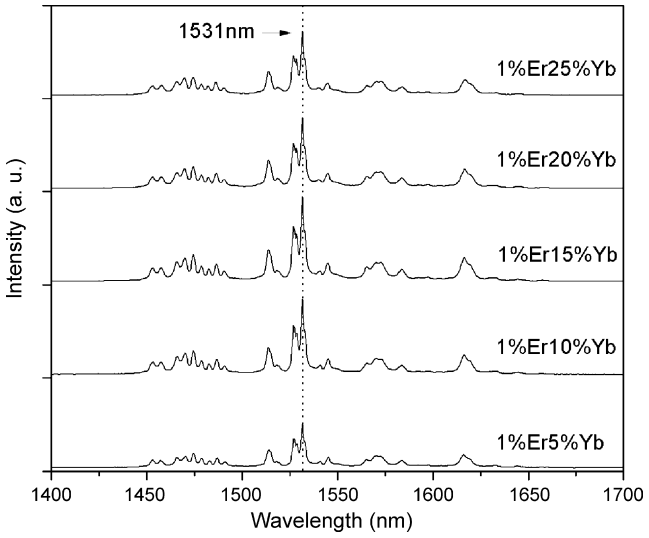

Fig. 7. The luminescence spectra of the Er,Yb:YAG ceramics in the infrared band excited by the 940 nm LD.

1%Er,5%Yb:YAG ceramic is about 15 μm, and those of the Er,Yb:YAG ceramics with different Yb contents are similar. Owing to the poreless microstructure, the Er,Yb co-doped YAG ceramics possess excellent transparencies above 80% in the visible band and the infrared band. And the in-line transmittances of the five samples with 1%Er–5%Yb, 1%Er–10%Yb, 1%Er–15%Yb, 1%Er–20%Yb and 1%Er–25%Yb are 82.9%, 84.1%, 83.2%, 83.9% and 83.5% respectively at 2000 nm, as shown in Fig. 3. Fig. 4 shows the corresponding absorption coefficient curves of these samples. From Figs. 3 and 4, it also can be seen that the absorption peaks centered at 940 and 968 nm are intensified dramatically along with the increasing addition of Yb. In this case the absorption saturation will be achieved easily. It also implies that Yb^{3+} ions have taken the place of Y^{3+} ions successfully owing to the similar chemical properties and ionic radii of Yb^{3+} (0.985 Å) and Y^{3+} (1.019 Å), which are from the same subgroup IIIB.

The upconversion mechanism of Er^{3+} and the energy transfer scheme between Er^{3+} and Yb^{3+} in optical materials are shown in Fig. 5. The $^2F_{5/2}$ level of Yb^{3+} and $^4I_{11/2}$ level of Er^{3+} have similar energy values, so Yb^{3+} ions can act as donors and Er^{3+} ions can be treated as acceptors. Fig. 6 shows the upconversion spectra of the samples in the visible band under the excitation of 940 nm LD. The green emissions and red emissions are centered at 553, 560, 671 and 678 nm respectively. In the upconversion scheme of Er^{3+} ions [19], the electrons at ground state $^4I_{15/2}$ can be excited to $^4I_{11/2}$ pumped by the 940 nm LD through ground state absorption (GSA), then through excited state absorption (ESA): $^4I_{11/2} \rightarrow {}^4F_{7/2}$ or energy transfer (ET): $^4I_{11/2} \rightarrow {}^4I_{15/2}$, $^4I_{11/2} \rightarrow {}^4F_{7/2}$, followed by fast cascading relaxation from $^4F_{7/2}$ to the $^2H_{11/2}/{}^4S_{3/2}$, and the green emissions are yielded through the transitions of $^2H_{11/2}/{}^4S_{3/2} \rightarrow {}^4I_{15/2}$. The yielding processes of the red emissions are firstly GSA: $^4I_{15/2} \rightarrow {}^4I_{11/2}$, followed by fast cascading relaxation to $^4I_{13/2}$, secondly ET: $^4I_{11/2} \rightarrow {}^4I_{15/2}$, $^4I_{13/2} \rightarrow {}^4F_{9/2}$, and finally $^4F_{9/2} \rightarrow {}^4I_{15/2}$. Fig. 7 shows the

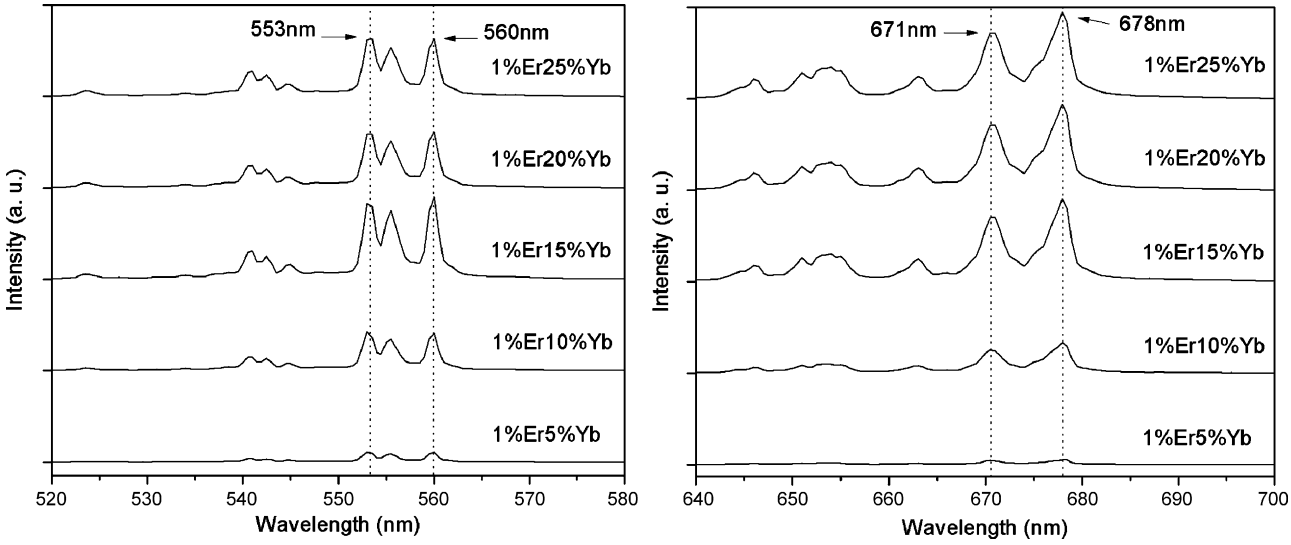

Fig. 6. The upconversion luminescence spectra of the Er,Yb:YAG ceramics in the visible band under excitation of the 940 nm LD.

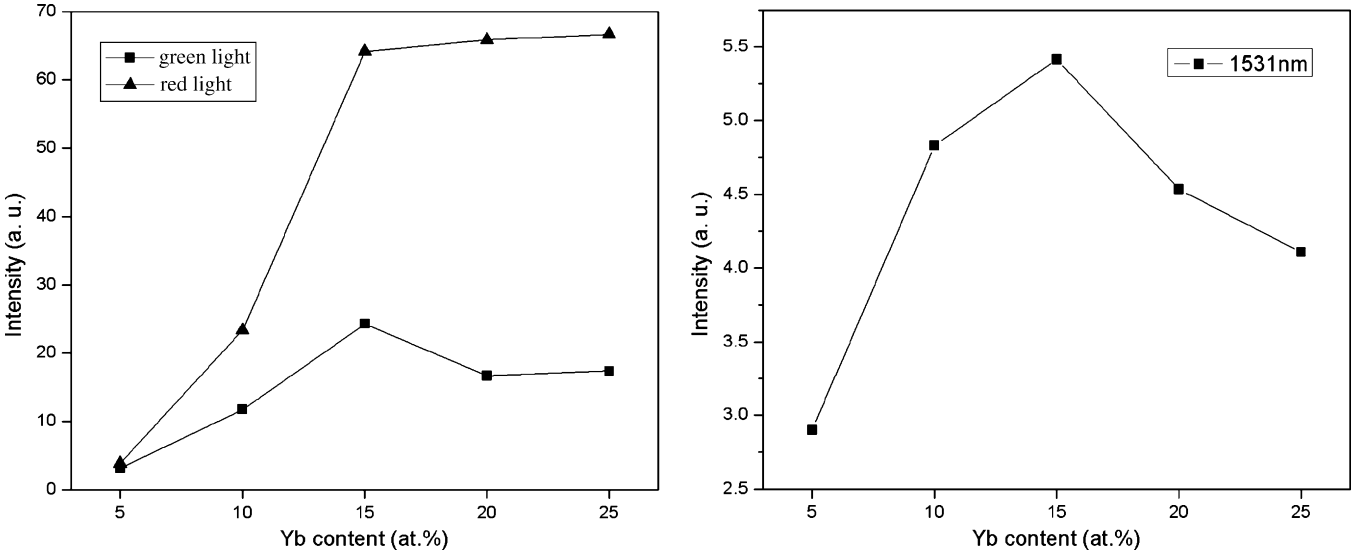

Fig. 8. The dependence of the luminescence intensities on Yb contents in the Er,Yb:YAG ceramics.

luminescence spectra of the samples in the infrared band excited by the 940 nm LD. Through the transition of $^4I_{13/2} \rightarrow {}^4I_{15/2}$, Er^{3+} ions can emit large band of lights from 1450 nm to 1650 nm because of energy level Stark splitting. The luminescence of 1531 nm is obviously dominant in the band and can be chosen as the aim of the laser experiment in the future.

It can be seen from Fig. 8 that the intensities of the green, red and infrared emissions all increase along with the more addition of Yb element and the increasing absorption to the 940 nm LD. The absorption saturation is achieved when the content of Yb exceeds 15%, and luminescence quenching occurs simultaneously for the infrared (centered at 1531 nm) and the green (centered at 553 and 560 nm) luminescence. So the addition of Yb element must have a limitation. When the content of Yb exceeds the upper limit, more ions and photons will be involved and the ET processes between the ions will become dominant. The red emissions depend on the ET processes [20]: $^4I_{11/2} \rightarrow {}^4I_{15/2}$, $^4I_{13/2} \rightarrow {}^4F_{9/2}$. That is why luminescence quenching seems to have little influence on the red emissions, not as on the green emissions and the infrared emissions. On the contrary, the intensities of the red emissions even increase slightly regardless of the absorption saturation when the content of Yb exceeds 15%. Therefore, for 1%Er doped YAG ceramics laser experiment, the best ion ratio of Yb^{3+} and Er^{3+} is around 15:1.

Fig. 9 reveals that the luminescence intensities increase proportionally along with the increase of the output power of the 940 nm LD. The luminescence of 1030 nm comes from the $^2F_{5/2} \rightarrow {}^2F_{7/2}$ transition in Yb^{3+}. The slopes (n), calculated by linearly fitting the upconversion luminescence intensity as a function of the LD power, indicates that one photon absorption process is involved in the infrared luminescence mechanism ($n = 1.03$ for the $^2F_{5/2} \rightarrow {}^2F_{7/2}$ transition in Yb^{3+}; $n = 1.12$ for the $^4I_{13/2} \rightarrow {}^4I_{15/2}$ transition in Er^{3+}). It also implies that the

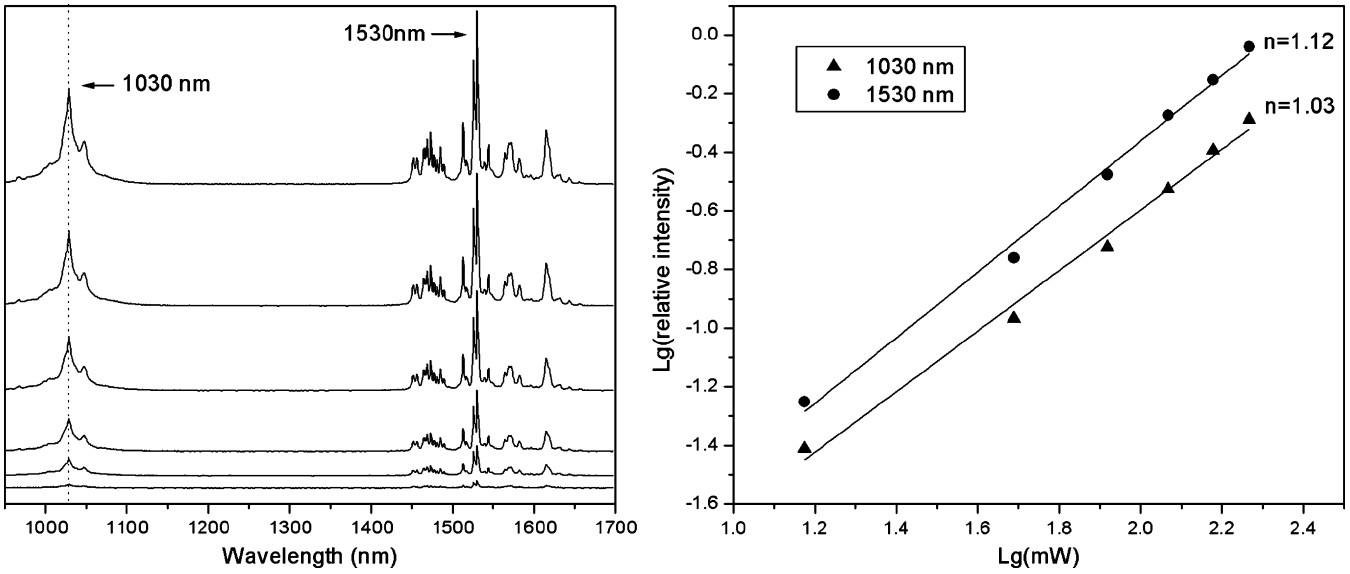

Fig. 9. The linear fitting between the logarithm of infrared luminescence intensities in 1%Er,15%Yb:YAG transparent ceramics and 940 nm LD output power (LD output power from up to down: 2.27, 2.18, 2.07, 1.92, 1.69 and 1.17 mW).

energy transfer scheme between Er^{3+} and Yb^{3+} is steady along with the increasing excitation power.

Fig. 10 shows the luminescence decay curves at 1531 nm in the Er:YAG and Er,Yb:YAG ceramics pumped by the 940 nm LD. It can be seen that the curves of Er,Yb:YAG ceramics show a rise at the early times because the Er^{3+} ions can accept energy from Yb^{3+} ions through the DT process from $^2F_{5/2}$ level of Yb^{3+} to $^4I_{11/2}$ level of Er^{3+}. Along with the increasing addition of Yb,

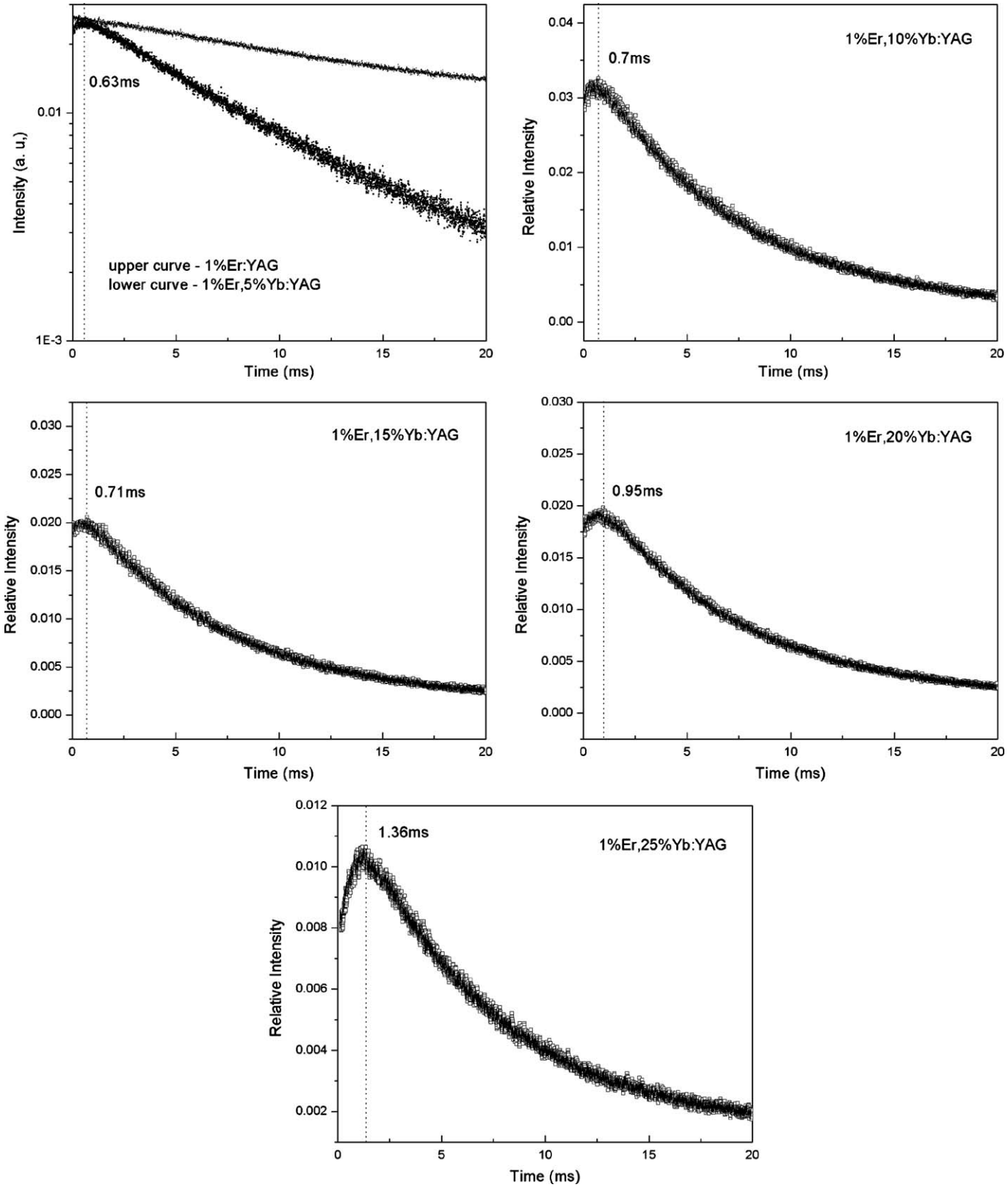

Fig. 10. The luminescence decay curves at 1531 nm in the Er:YAG and Er,Yb:YAG ceramics.

Table 1
The luminescence lifetime values of Er,Yb:YAG transparent ceramics at 1531 nm and 1030 nm respectively.

Er,Yb contents (at.%)	Lifetime at 1531 nm (ms)	Lifetime at 1030 nm (ms)
1%Er	14.61 ± 4.54E−5[a]	–
1%Er–5%Yb	7.36 ± 9.28E−6	0.49 ± 9.38E−7
1%Er–10%Yb	7.28 ± 7.88E−6	0.56 ± 1.23E−6
1%Er–15%Yb	7.28 ± 1.16E−5	0.65 ± 1.68E−6
1%Er–20%Yb	7.27 ± 8.93E−6	0.69 ± 5.72E−7
1%Er–25%Yb	7.17 ± 1.49E−5	0.72 ± 5.69E−6

[a] Standard error.

more and more Yb^{3+} ions can act as donors to provide energy for Er^{3+} ions, so the rise processes will continue for longer time accordingly. The lasting times of the rise processes of the ceramics with 1%Er–5%Yb, 1%Er–10%Yb, 1%Er–15%Yb, 1%Er–20%Yb and 1%Er–25%Yb are 0.63, 0.70, 0.71, 0.95 and 1.36 ms respectively. And measured by the exponential decay fitting, the 1531 nm luminescence lifetimes of these ceramics seem to show a trend of decreasing along with the increasing addition of Yb element, and the 1030 nm lifetimes show a trend of increasing along with the increasing addition of Yb element, as shown in Table 1. As we know, during the energy transfer process, Yb^{3+} ions could also be the acceptors, while Er^{3+} ions act as the providers. Although more Yb^{3+} ions could provide more energy to Er^{3+} ions theoretically, it also means more Yb^{3+} ions could accept the energy from Er^{3+} ions. So Yb^{3+} ions will limit the maximum population in $^4I_{11/2}$ level of Er^{3+} ions. Therefore, when doping 5%Yb into the 1%Er:YAG ceramic, the 1531 nm luminescence lifetime drops from 14.61 ms to 7.36 ms dramatically, and then along with the increasing addition of Yb, it shows a trend of decreasing. Since 1531 nm luminescence lifetimes of the ceramics with 1%Er–10%Yb, 1%Er–15%Yb and 1%Er–20%Yb doped are very similar, the proper atomic ratio of Yb and Er element should not exceed 20:1. It dovetails with the conclusion mentioned above – for 1%Er doped YAG ceramics laser experiment, the best ion ratio of Yb^{3+} and Er^{3+} is around 15:1.

4. Conclusions

In this study, the transparent polycrystalline Er,Yb:YAG ceramics with various Yb contents from 5% to 25% were prepared by the solid-state reaction and the vacuum-sintering technique. The in-line transmittances of the mirror-polished Er,Yb:YAG ceramics exceed 80% from the visible band to the infrared band. The samples are very compact with few pores. The average grain size of the Er,Yb:YAG ceramic is about 15 μm. The luminescence quenching occurs when Yb content exceeds 15%. The luminescence decay curves of the Er,Yb:YAG ceramics show the rise processes at the early times because the Er^{3+} ions can accept energy from Yb^{3+} ions through the DT process from $^2F_{5/2}$ level of Yb^{3+} to $^4I_{11/2}$ level of Er^{3+}. And the luminescence lifetimes show a trend of decreasing along with the increasing addition of Yb element, while the 1030nm lifetimes show a trend of increasing. It was concluded that Yb^{3+} ions could limit the maximum population in $^4I_{11/2}$ level of Er^{3+} ions. For 1%Er doped YAG ceramic laser experiment, the best ion ratio of Yb^{3+} and Er^{3+} is around 15:1.

Acknowledgements

This work was supported by the 863 project (No. AA03Z523), National Science Foundation (No. 50990300), the Natural Science Foundation of Shanghai (No.10ZR1433900) and the Major Basic Research Programs of Shanghai (No. 07DJ14001).

References

[1] T. Danger, G. Huber, K. Petermann, W. Seeber, Dependence of the 1.6 μm laser performance on the composition of Yb, Er-doped fluoride phosphate glasses, in: Proc. OSA, Advanced Solid State Laser Conf. (ASSL), 1998, 305–307.
[2] F. Song, M.J. Myers, S. Jiang, Y. Feng, X.B. Chen, G.Y. Zhang, Effect of erbium concentration on upconversion luminescence of Er:Yb:phosphate glass excited by InGaAs laser diode, in: S. Jiang, S. Honkanen (Eds.), Rare-Earth-Doped Materials and Devices III, Proc. SPIE, vol. 3622, 1999, 182–188.
[3] E. Georgiou, O. Musset, J.P. Boquillon, High-efficiency and high-output pulse energy performance of a diode-pumped Er:Yb:glass 1.54-μm laser, Appl. Phys. B 70 (2000) 755–762.
[4] E. Georgiou, O. Musset, J.P. Boquillon, B. Denker, S.E. Sverchkov, 50 mJ/30 ns FTIR Q-switched diode-pumped Er:Yb:glass 1. 54-μm laser, Opt. Commun. 198 (2001) 147–153.
[5] F. Meng, F. Song, C. Zhang, X. Ding, M. Shang, G. Zhang, Laser diode pumped 1.54 μm Er:Yb:phosphate glass continuous wave compact laser, Chin. Phys. Lett. 20 (2003) 1739–1740.
[6] F. Song, S. Liu, Z. Wu, H. Cai, J. Su, J. Tian, J. Xu, Model of longitudinally laser diode pumped erbium ytterbium-codoped phosphate glass microchip laser with upconversion, J. Quantum Electron. 43 (2007) 817–823.
[7] A. Ikesue, T. Kinoshita, K. Kamata, K. Yoshida, Fabrication and optical properties of high-performance polycrystalline Nd:YAG ceramics for solid-state lasers, J. Am. Ceram. Soc. 78 (1995) 1033–1040.
[8] T. Yanagitani, H. Yagi, M. Ichikawa, Japanese Patent 10-101333 (1998).
[9] J. Lu, M. Prabhu, J. Xu, K. Ueda, H. Yagi, T. Yanagitani, A.A. Kaminskii, Highly efficient 2% Nd:yttrium aluminum garnet ceramic laser, Appl. Phys. Lett. 77 (2000) 3707–3709.
[10] J. Lu, T. Murai, K. Takaichi, T. Uematsu, K. Misiwa, M. Prabhu, J. Xu, K. Ueda, H. Yagi, T. Yanagitani, A.A. Kaminskii, A. Kudryashov, 72 W Nd:$Y_3Al_5O_{12}$ ceramic laser, Appl. Phys. Lett. 78 (2001) 3586–3588.
[11] J. Lu, H. Yagi, K. Takaichi, T. Uematsu, J. Bisson, Y. Feng, A. Shirakawa, K. Ueda, T. Yanagitani, A.A. Kaminskii, 110 W ceramic Nd^{3+}:$Y_3Al_5O_{12}$ laser, Appl. Phys. B 79 (2004) 25–28.
[12] Y. Wu, J. Li, Y. Pan, Q. Liu, J. Guo, B. Jiang, J. Xu, Diode-pumped passively Q-switched Nd:YAG ceramic laser with a Cr^{4+}:YAG crystal satiable absorber, J. Am. Ceram. Soc. 90 (2007) 1629–1631.
[13] Y. Wu, J. Li, Y. Pan, J. Guo, B. Jiang, Y. Xu, J. Xu, Diode-pumped Yb:YAG ceramic laser, J. Am. Ceram. Soc. 90 (2007) 3334–3337.
[14] J. Li, Y. Wu, Y. Pan, W. Liu, L. Huang, J. Guo, Fabrication, microstructure and properties of highly transparent Nd:YAG laser ceramics, Opt. Mater. 31 (2008) 6–17.
[15] J. Li, Y. Wu, Y. Pan, W. Liu, L. Huang, J. Guo, Laminar-structured YAG/Nd:YAG/YAG transparent ceramics for solid-state lasers, Int. J. Appl. Ceram. Technol. 5 (2008) 360–364.
[16] W. Zhang, Y. Pan, J. Zhou, W. Liu, J. Li, B. Jiang, X. Cheng, J. Xu, Diode-pumped Tm:YAG ceramic laser, J. Am. Ceram. Soc. 92 (2009) 2434–2437.
[17] W.-X. Zhang, J. Li, W.-B. Liu, Y.-B. Pan, J.-K. Guo, Fabrication and properties of highly transparent $Tm_3Al_5O_{12}$ (TmAG) ceramics, Ceram. Int. 35 (7) (2009) 2927–2931.

[18] E. Georgiou, F. Kiriakidi, O. Musset, J.P. Boquillon, 1.65-μm Er:Yb:YAG diode-pumped laser delivering 80-mJ pulse energy, Opt. Eng. 44 (2005) 064202-1–164202-10.
[19] J. Zhou, W. Zhang, J. Li, B. Jiang, W. Liu, Y. Pan, Upconversion luminescence of high content Er-doped YAG transparent ceramics, Ceram. Int. 36 (2010) 193–197.
[20] R.R. Gonçalves, G. Carturan, L. Zampedri, M. Ferrari, A. Chiasera, M. Montagna, G.C. Righini, S. Pelli, S.J.L. Ribeiro, Y. Messaddeq, Infrared-to-visible CW frequency upconversion in erbium activated silica-hafnia waveguides prepared by sol–gel route, J. Non-Cryst. Solids 322 (2003) 306–310.